



Entergy Operations, Inc.
1448 S.R. 333
Russellville, AR 72802
Tel 501 858 5000

1CAN120302

December 31, 2003

U.S. Nuclear Regulatory Commission
Attn: Document Control Desk
Washington, DC 20555

SUBJECT: Supplement to Amendment Request
To Changes to the Spent Fuel Pool Loading Restrictions
Arkansas Nuclear One, Unit 1
Docket No. 50-313
License No. DPR-51

- REFERENCES:
1. Entergy letter to the NRC dated April 2, 2003, "License Amendment Request to Modify the Fuel Assembly Enrichment, the Spent Fuel Pool (SFP) Boron Concentration Technical Specification (TS) 3.7.1.4, the Loading Restrictions in the SFP in TS 3.7.15, and to Modify the Fuel Storage Design Features in TS 4.3" (1CAN040302)
 2. Entergy letter to the NRC dated November 21, 2003, "Supplement to Amendment Request To Changes for the Spent Fuel Pool Loading Restrictions (1CAN110302)

Dear Sir or Madam:

By letter (Reference 1), Entergy Operations, Inc. (Entergy) proposed a change to the Arkansas Nuclear One, Unit 1 (ANO-1) Technical Specifications (TSs) to modify the fuel assembly enrichment and the spent fuel pool (SFP) loading restrictions.

By letter (Reference 2), Entergy responded to questions from the Reactor Systems Branch, the Materials and Chemical Engineering Branch, the Mechanical and Civil Engineering Branch, and the Plant Systems Branch. Entergy communicated in response to the questions from the Mechanical and Civil Engineering Branch that due to the redesign of the stainless steel frame, which provides the support structure for the Metamic panels, a new structural analysis was required. A summary of the new engineering analysis, which has been performed by Stevenson and Associates, is included as Attachment 1 to this letter. The Stevenson and Associates summary report replaces entirely the structural summary report that was submitted as Section 6.0 of Attachment 4, Holtec License Report, in Reference 1.

Attachment 2 to this letter contains minor changes based on the final design of the poison insert assembly to Sections 1.0, 2.0, and 3.0 of the Holtec License Report (Attachment 4 to Reference 1). Also included in Attachment 2 are minor changes to the Evaluation of Spent Fuel Pool Structural Integrity for Increased Loads from Spent Fuel Racks (Attachment 5 of

1001

Reference 1), replacing Holtec International with Stevenson and Associates as the performer of the structural analysis. Only the paragraphs that changed in each attachment are included. The changes are reflected with revision bars.

There are no technical changes proposed. The original no significant hazards consideration included in Reference 1 is not affected by any information contained in this supplemental letter. There are no new commitments contained in this letter.

If you have any questions or require additional information, please contact Dana Millar at 601-368-5445.

I declare under penalty of perjury that the foregoing is true and correct. Executed on December 31, 2003.

Sincerely,

A handwritten signature in black ink, appearing to read "Joseph A. Kowalewski". The signature is fluid and cursive, with a large initial "J" and a long, sweeping underline.

Joseph A. Kowalewski
Director, Engineering

JAK/dm

Attachments:

1. Stevenson and Associates Fuel Pool Rack Structural / Seismic Considerations
2. Revised Portions of Original Submittal (1CAN040302)

cc: Dr. Bruce S. Mallett
Regional Administrator
U. S. Nuclear Regulatory Commission
Region IV
611 Ryan Plaza Drive, Suite 400
Arlington, TX 76011-8064

NRC Senior Resident Inspector
Arkansas Nuclear One
P. O. Box 310
London, AR 72847

U. S. Nuclear Regulatory Commission
Attn: Mr. John L. Minns
MS O-7 D1
Washington, DC 20555-0001

Mr. Bernard R. Bevill
Director Division of Radiation
Control and Emergency Management
Arkansas Department of Health
4815 West Markham Street
Little Rock, AR 72205

Attachment 1

To

1CAN120302

Stevenson and Associates Fuel Pool Rack Structural / Seismic Considerations

6 STRUCTURAL/SEISMIC CONSIDERATIONS

6.1 Introduction

The overall design objectives of the spent fuel storage pool at Arkansas Nuclear One (ANO) Unit 1 are governed by various Regulatory Guides, the Standard Review Plan, and industry standards. This section addresses the structural adequacy of the Spent Fuel Pool (SFP) maximum density spent fuel racks at ANO Unit 1 with the poison inserts by evaluating this structural system using the appropriate regulatory and design standards. Postulated loadings for normal, seismic, and accident conditions at the ANO Unit 1 site are considered in this analysis and evaluation.

The design adequacy of the racks and the poison inserts, are confirmed with analyses that are performed in compliance with the USNRC Standard Review Plan [6.1.1], the USNRC Office of Technology Position Paper [6.1.2], Lawrence Livermore Report UCRL52342 [6.1.3] and ANO Specification APL-C-502 [6.1.4]. This report is a summary of the Ref. [6.1.5] detailed calculation performed to assess the design adequacy of the racks with the poison inserts. This report section includes a description of the rack layout in Subsection 6.2, the methodology used to analyze the rack structures in Subsection 6.3, the development of the SOLVIA Structural dynamic model in Subsection 6.4, the applicable load combinations in Subsection 6.5, a summary of all the analyses performed in Subsection 6.6, the acceptance criteria in Subsection 6.7, the analysis results in Subsection 6.8, Conclusions in Subsection 6.9 and References in Subsection 6.10.

6.2 Rack Layout and Description

6.2.1 Rack Layout Description

The ANO Unit 1 Spent Fuel Pool contains eight independent rack structures designed to hold the spent fuel assemblies and rod cluster control assemblies in storage for long term decay. There are three regions of racks. The Region 1 racks employ Boroflex as the poison material. Region 2 racks do not have any poison material. Region 3 racks are Region 2 racks that will be modified by inserting Metamic poison material strips into the flux trap component of some of the cells. The pool layout is illustrated in Figure 6.1, including the rack modules and the X and Y coordinate axes used in the model development.

The racks are free standing on fourteen feet that rest on the bottom of the pool. The eight racks, originally designed by Westinghouse, are self-supporting and are not connected to each other or to the SFP walls. There are two Region 1 racks, four Region 2 racks and two proposed Region 3 racks (that are modified Region 2 racks).

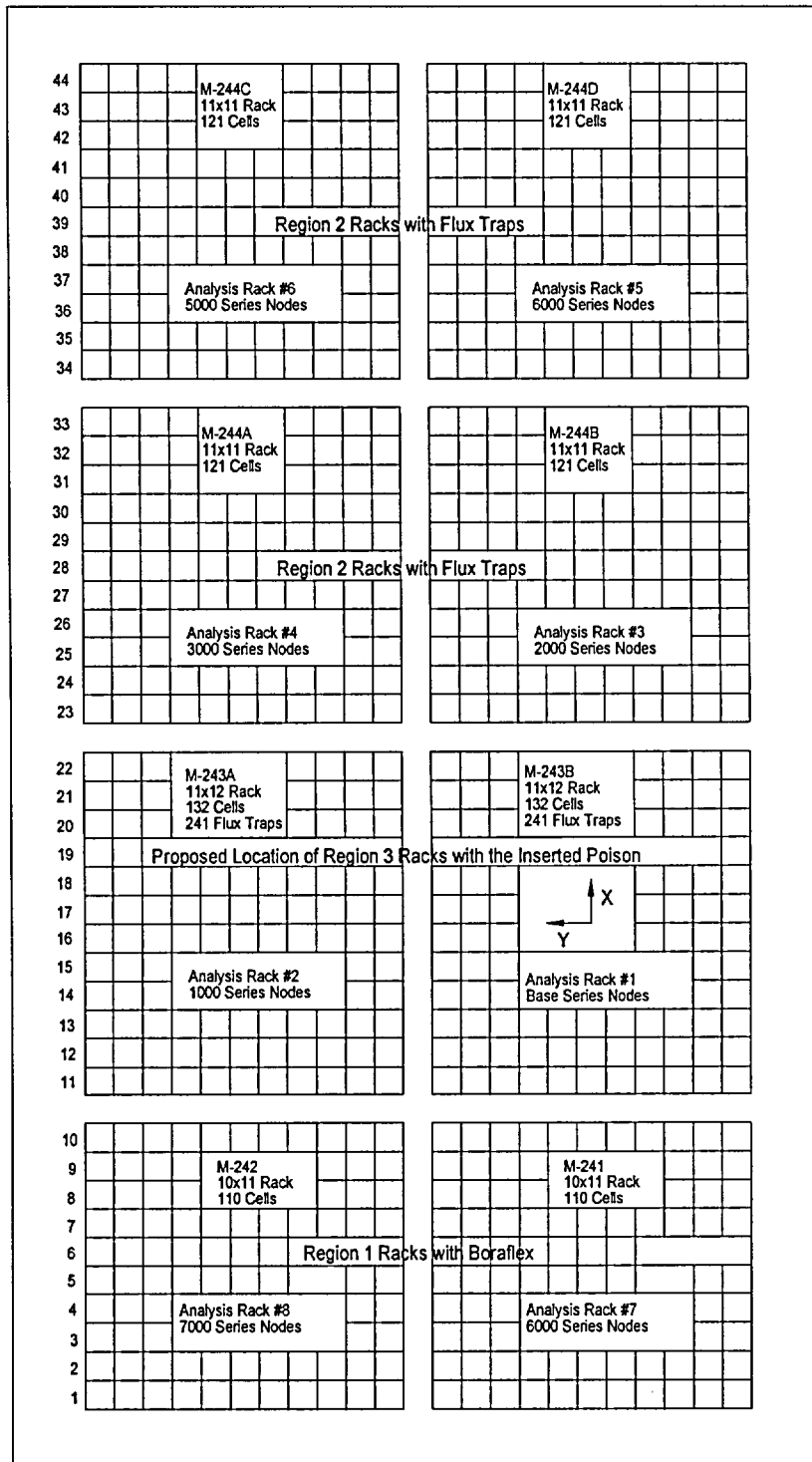


Figure 6.1 - ANO Unit 1 Spent Fuel Pool Layout

6.2.2 Material Properties of Rack, Fuel and Poison Inserts (Design Inputs)

The high density storage rack weights from Ref. [6.2.1] and are given in Table 6.2.1 below. The weights used in the analysis were within about 3% of the values below as discussed in Section 6.4.1.

Table 6.2.1			
RACK WEIGHT DATA			
Rack #	Cells/Module	Array Size	Empty Rack Dry Weight (lbs)
1 (Region 2)	121	11x11	17,650
2 (Region 2)	121	11x11	17,650
3 (Region 3)	132	11x12	19,150
4 (Region 1)	110	10x11	27,650
5 (Region 2)	121	11x11	17,650
6 (Region 2)	121	11x11	17,650
7 (Region 3)	132	11x12	19,150
8 (Region 1)	110	10x11	27,650

The racks are numbered 1 through 8. Rack #1 is in the northeast corner of the pool. The numbering progresses north to south and east to west, so that Rack #4 is in the southeast corner and Rack #8 is in the southwest corner.

The Cartesian coordinate system utilized within the rack dynamic model has the following nomenclature:

- X = Horizontal axis along plant South
- Y = Horizontal axis along plant East
- Z = Vertical axis upward from the rack base

The material properties for the rack and support material are summarized in Table 6.2.2 below.

Table 6.2.2			
RACK MATERIAL DATA (ASME – Section II, Part D)			
MATERIAL DATA (T _o = 150°F)			
Stainless Steel Material	Young's Modulus E (psi)	Yield Strength S _y (psi)	Tensile Strength S _u (psi)
SA240, Type 304	27.7 x 10 ⁶	27,500	73,000
SA479, Type 304	27.7 x 10 ⁶	27,500	73,000
MATERIAL DATA (T _a = 250°F)			
SA240, Type 304	27.3 x 10 ⁶	23,750	68,500
SA479, Type 304	27.3 x 10 ⁶	23,750	68,500

6.3 Rack Analysis Methodology

6.3.1 Overview of Rack Structural Analysis Methodology

The response of a free-standing rack module to seismic loadings is nonlinear and involves a complex combination of motions (rocking, twisting, turning and sliding). This could potentially cause impacts within the structure (fuel assemblies to the cell walls) and between modules. Rack dynamic behavior includes a large portion of the total structural mass in a confined rattling motion. The rack pedestals are restricted from lateral motion only by friction at the base. In addition, there are large fluid coupling effects due to water around the assemblies and the independent adjacent structures.

Linear dynamic analysis methods cannot reasonably simulate the structural response of these highly nonlinear structures when subjected to earthquake loadings. An appropriate simulation can only be obtained by direct integration of the nonlinear equations of motion with three directional pool slab acceleration time-histories applied as forcing functions acting on the structures simultaneously.

Whole Pool Multi-Rack (WPMR) analysis is used to obtain final analysis results in order to simulate the dynamic behavior of the storage rack structures. This subsection provides methodology used in the analysis.

6.3.2 Analysis Methodology Background

Reliable assessment of stresses within the rack components and stored fuel behavior within the rack modules requires a dynamic model that incorporates the appropriate

Stevenson & Associates Report 03Q3428-01

attributes of the actual structure. The model must feature the ability to simultaneously simulate concurrent motions compatible with the rack and fuel storage installation.

The model has the capability to affect interactions, which occur due to rattling of fuel assemblies inside storage cells, and lift-off of the support pedestals on the pool floor. The contribution of the water mass in the spaces around the rack modules and within the storage cells is modeled in an accurate manner.

The friction coefficient at the pedestal-to-pool liner (or bearing pad) interface may lie in a rather wide range and a conservative value of friction cannot be prescribed without performing bounding simulations. Different friction coefficients provide the governing results for different analysis parameters. For example, the lower bound friction results in the largest overall rack displacement which may seem obvious, however other parameters such as largest impact force between the rack and fuel assembly being largest with the upper bound friction is a result not immediately predictable.

The approach used in this evaluation was to develop single rack models for the region 3 type rack structure, since these are the ones being modified relative to the current seismic qualification analysis (Reference 1). The three-dimensional single rack dynamic model addresses the parameters discussed above. Single rack simulations are not by themselves appropriate in determining the maximum dynamic response. This is due to the participation of water around the racks, with hydraulic interaction that may either increase or decrease rack motion. The results of this evaluation confirm that the dynamics of one rack affects the motion of the others in the pool. Therefore, the dynamic simulation of one rack, while providing a great deal of insight into this behavior, may not adequately predict the motion or structural response (applied forces and internal stresses) of rack modules.

For this reason, the hydraulic and dynamic interaction of closely spaced racks is simulated by including all modules in one comprehensive simulation using a WPMR model. All rack modules are modeled simultaneously and the coupling effect due to multi-body motion is included in the analysis. Region 2 rack models for the whole pool model were developed from the Region 3 rack model with corrections for one less row of cells. The Region 2 and Region 3 racks are identical except for the number of rows of cells. Similarly, the Region 1 rack models for the whole pool model were developed from the Region 3 rack model, with appropriate changes to section properties due to the differences in cell cross-section and additional framing members present in the Region 1 racks.

6.3.2.1 Equation of Motion

Program SOLVIA was used for the dynamic non-linear time history analysis of the single rack and WPMR model of the structures. Using the direct time integration method, the equations of motion are solved at each time step for acceleration time histories in each of the three degrees of freedom. The basic equations that SOLVIA is operating on are:

$$M\ddot{U}(t) + C\dot{U}(t) = R(t) - F(t)$$

where:

- M = constant mass matrix,
 - C = constant damping matrix,
 - $R(t)$ = external load vector applied at time t ,
 - $F(t)$ = nodal point force vector equivalent to the element stresses at time t ,
- A superimposed dot denotes time derivative, e.g.,
- $\dot{U}(t)$ = nodal point velocity vector at time t .
 - $\ddot{U}(t)$ = nodal point acceleration vector at time t .

An implicit time integration method is employed for this structural vibration problem.

There are several non-linear attributes and unique hydrodynamic properties of this structure that are modeled. The model has been built by modeling each attribute and checking their effects one at a time. Each single rack model is developed by appropriately combining these attributes. The WPMR is modeled by combining the eight modules and including the appropriate off diagonal stiffness matrix and mass matrix terms that include the interactions between the modules.

6.3.2.2 Friction Coefficient Between Rack Supports and Pool Floor

It is not possible to determine an accurate coefficient of friction (μ) between the pedestal supports and the pool floor. Data on austenitic stainless steel plates submerged in water show a mean value of μ to be 0.503 [Ref. 6.3.3] with a standard deviation of 0.125. Upper and lower bounds (based on twice the standard deviation) are 0.753 and 0.253, respectively. Therefore, coefficient of friction values of 0.2 (lower limit) and 0.8 (upper limit) as well as a best estimate value of 0.5 provide reasonable limits and should provide a reasonable envelope for calculating the upper bound module response for each design parameter.

The friction interface between rack support pedestal and liner in the fuel rack simulations is simulated by linear contact (friction) elements. These elements function only when the pedestal is physically in contact with the pool floor. Friction elements are also included

at the base of the fuel rod to rack base interface to reasonably model the behavior of the rod at this juncture. The coefficient of friction modeled at this interface was consistent with that used for the pedestal/pool bottom interface for a given analysis.

6.3.2.3 Rack Beam Behavior

The structural model using an equivalent beam stiffness developed for the full cell structure, was modeled using linear beam members to represent the elastic bending and twisting action.

The equivalent moment of inertia for the beam was estimated using a shell element model of a row of cells with the appropriate number of cells included for each horizontal direction. The axial area was estimated using a single cell model. The overall combined section properties for each type of rack module were then estimated from results of analysis of these models for applied unit displacements.

6.3.2.4 Impact Behavior

To include the impact behavior, compression-only gap elements are used to provide for opening and closing of interfaces such as the pedestal-to-pool floor interface and the fuel assembly-to-cell wall interface. These interface gaps are modeled using nonlinear spring elements (Gapped Truss elements in SOLVIA). The nonlinear spring is the mathematical representation of the condition where a restoring force is zero until the gap is closed and then is linearly proportional to displacement.

6.3.2.5 Fuel Loading to Cell Wall Behavior

The fuel assemblies are conservatively assumed to rattle in unison which provides an upper bound for the contribution of impact against the cell wall. This is modeled with a single spent fuel assembly which is a combination of all the assemblies contained in the rack. This single assembly is allowed to rattle against the wall of the equivalent beam element. This results in the impact load being a combination of all 132 fuel assemblies hitting the wall at the same time.

From Reference 6.1.3, it is noted that impact damping is a significant source of damping for multiple impacting members. The same effective damping due to fuel to cell impact as a function of mass and stiffness presented in Reference 6.3.1 was used. From Reference 6.3.1, the damping coefficient was calculated as:

$$C = 2 \times \text{damping} \times \sqrt{Km} * A_f$$

where C = effective damping coefficient
K = impact stiffness
m = mass
A_f = area
damping = 2%

6.3.2.6 Fluid – Rack Coupling

The WPMR model used for this analysis handles simultaneous simulation of all racks in the pool as a WPMR three dimensional analysis. The WPMR analysis is appropriate for predicting maximum structural stresses with reasonable predictions of rack dynamic response.

During an earthquake, all racks in the pool are subject to the input excitation simultaneously. While the possibility of inter-rack impact is not a common occurrence and depends on rack spacing, the effect of water (the fluid coupling effect) is a factor. It is, therefore, essential that the contribution of the fluid forces be included in a comprehensive manner. This is possible when all racks in the pool are included in a three dimensional simulation using a mathematical model that includes all modules moving simultaneously. The fluid coupling effect encompasses interaction between every set of racks in the pool. The motion of one rack effects the fluid forces on all other racks and on the pool walls. Therefore, both near-field and far-field fluid coupling effects are included in the analysis.

6.3.3 Poison Insert Analysis Methodology

The poison inserts are analyzed together with the rack and spent fuel assemblies by including them in the structural model. The poison inserts are included with the rack members by calculating their contribution to the overall mass and stiffness of the beam members and lumped masses of the composite model. The forces (resulting primarily from accelerations) acting on individual inserts are calculated by computing the proportional share of the force from the applied accelerations on the overall rack module models.

The local response of the inserts was checked using manual calculations. In-structure time-histories at the top of the Region 3 racks were extracted for the case with the highest acceleration response. In-structure response spectra were developed from these time histories, and the inserts were evaluated using these response spectra.

6.3.4 Whole Pool Multi-Rack (WPMR) Methodology

The WPMR analysis must deal with both stress displacement and impact criteria. The model development and analysis steps that are undertaken are summarized in the following steps.

- a. The section and mass properties of a single cell are developed.
- b. Using the single cell section and mass properties, equivalent properties for each rack module are developed.
- c. Similarly, single element properties are calculated for the fuel assembly, poison inserts and the base pedestals. These are also used to develop equivalent properties for the rack module.

- d. Individual stiffness used in the gap elements are calculated for each of the interfaces included in the model. These include the pedestal base to pool floor, rack to rack and rack to wall stiffness and fuel assembly to rack wall interface. These are also appropriately combined to get equivalent module properties.
- e. Calculate the appropriate hydrodynamic properties for the spent fuel assemblies and rack. This includes the hydrodynamic mass and the off-diagonal hydrodynamic mass matrix terms.
- f. Develop the individual or single rack models in the pool.
- g. Combine the single rack models into one three-dimensional dynamic model suitable for a time-history analysis of the racks. These models include the assemblage of all rack modules in the pool. Include all fluid coupling interactions and mechanical coupling appropriate to performing an accurate non-linear simulation.
- h. Perform the three-dimensional dynamic analyses on various physical conditions (such as coefficient of friction and extent of cells containing fuel assemblies). Archive the appropriate displacement and load outputs from the dynamic model for post-processing.
- i. Using the force and moment outputs from the dynamic analyses, perform stress analysis of high stress areas for the limiting cases. Use simple modeling techniques to evaluate the local regions of the structure that need to be evaluated. Demonstrate compliance with ASME Code Section III, Subsection NF limits on stress and displacement.

6.4 Rack Model Development

6.4.1 Single Rack Module Development

The Region 3 rack includes 11 by 12 cells. The weight of each component from Reference 6.2.1 is as follows:

Rack weight = 19,150 lb

Fuel weight = 1,700 lb* 132 Assemblies = 224,400 lb

Inserted Poison Panels = 100 lb * 241 = 24,100 lb

Total weight (dry) = 267,650 lb

In order to verify the Region 3 rack weight the weight was estimated using the actual mass densities and using the structural drawings. The weight of the various structure components were calculated as follows:

Base plate $W_{bp} = 128.8 \times 118.5 \times 0.5 \times 0.29 = 2.213 \times 10^3$ lb

Rack walls $W_{rw} = 373.256 \times 162 \times 0.29 = 17,540$ lb

Stevenson & Associates Report 03Q3428-01

Total $W_R = 17,540 + 2,210 = 19,750$ lb

Although the total weight is close to the 19,150 lb weight from Ref. [6.2.1] (within about 3%) a weight of 19,750 lb calculated above was used in the analysis for the Region 3 racks. Using the same method 18,100 lb was calculated and used in the analysis for the Region 2 racks. The weight of the Region 1 racks was not verified however, based on the verification above, the 27,650 lb weight from Ref. [6.2.1] was justified and used.

The material properties for the stainless steel rack used in the analysis are as follows:

Type 304 A240 18CR – 8N (Ref. 6.6.2):

Modulus of Elasticity, $E_s = 27.7 \times 10^6$ psi

Poisson's Ratio $\mu_s = 0.3$ (Steel)

Density (Stainless Steel--weight units) $\delta_{(w)} = 0.29$ lb/in³

The material properties used for the pool concrete from Ref. 6.8.2 are as follows:

Compressive Strength, $f_c' = 4000$ psi

Modulus of Elasticity, $E_c = 57000\sqrt{f_c'} = 57000\sqrt{4000}$ psi = 3.60E6 psi

Poisson's Ratio $\mu_c = 0.16$ (Concrete)

Density (Concrete--weight units) $\delta_{(w)} = 0.0868$ lb/in³

Fuel weight $W_f = 1700$ lb (assume the weight is uniformly distributed)

The Single Rack combined structural section properties [Moment of Inertias (I_x and I_y) and Area, A] for the Region 2 and 3 modules are as follows:

$$I_x = 256,670 \text{ in}^4$$

$$I_y = 234,960 \text{ in}^4$$

$$A = 373.256 \text{ in}^2$$

The stiffness for the Gap compression only element at the base is as follows:

$$K_{ped} = 1.16 \times 10^7 \text{ lb/in.}$$

6.4.2 Single Rack to Multi-Rack Model Development

The single rack models are combined into the WPMR model and the inter-rack gap stiffness springs are attached. When the gaps are closed the following stiffness in Table 6.4.1 will be in effect between these interfaces:

Impact Spring Type	Spring Constant [lb/in]
Rack to Rack (top)	2.82 E5
Rack to Rack (bottom)	1.01 E6
Rack to Pool Wall (top)	2.75 E5
Rack to Pool Wall (bottom)	9.25 E5
Fuel to Rack	1.9 E6 (Note 1)

Note 1 – The fuel to rack stiffness includes the influence of the Poison Insert Wedge (see Subsection 6.4.3.5) and is a summation of all the fuel to rack stiffness of each fuel assembly in each individual cell. This local stiffness without the wedge is 6.5×10^4 lb/in.

6.4.3 Model Details and Description

The rack structure dynamic model was prepared by considering nonlinearities and parametric variations. Particulars of modeling details and assumptions for the WPMR analysis of racks are given in the following subsections.

6.4.3.1 Modeling Details and Assumptions

- a. The model for the rack is supported at the base level, on four (corner) pedestals, modeled using non-linear compression-only gap spring elements and eight linear friction spring elements. These elements are located with respect to the centerline of the rack beam to allow for arbitrary rocking and sliding motions.
- b. The fuel rack structure motion is simulated by modeling the rack using 6 degrees-of-freedom at each mass point of the model. This includes the displacements and rotations at each of these points. The response of the module relative to the base is simulated in the dynamic analyses using suitable springs to couple the rack degrees-of-freedom and simulate rack stiffness.
- c. Fluid coupling between the rack and fuel assemblies and between the rack and wall is simulated by appropriately modeling of the off diagonal mass matrix terms. Inclusion of these effects uses rack/assembly coupling and rack-to-rack coupling as described in subsection 6.4.3.3.
- d. Fluid damping and velocity drag due to water particle velocity are not modeled. These effects are considered implicitly in the fluid coupling and fluid assumption mass modeling described in c. and i.
- e. Rattling fuel assemblies within the rack are modeled by five lumped masses located at H, 0.75H, 0.5H, 0.25H, and at the rack base (H is the rack height measured above the base-plate). Each lumped fuel mass has two horizontal displacement degrees-of-freedom. Vertical motion of the fuel assembly mass is assumed equal to rack vertical motion at the base-plate level.

- f. Seismic motion of a fuel rack is characterized assuming that fuel assemblies in their individual storage location move together in phase. This is the worst case computed dynamic loading on the rack structure for this phenomenon.
- g. Potential impacts between the cell walls of the racks and the contained fuel assemblies are accounted for by appropriate compression-only gap elements between the masses involved. The possible incidence of rack-to-wall or rack-to-rack impact is simulated by gap elements at the top and bottom of the rack in two horizontal directions. Bottom gap elements are located at the base-plate elevation. The initial gaps reflect the presence of base-plate extensions, and the rack stiffnesses are chosen to simulate the local structural detail.
- h. Pedestals are modeled using gap elements in the vertical direction and as “rigid links” for transferring horizontal forces. Each pedestal support is linked to the pool liner (or bearing pad) by two friction springs. The spring rate for the friction springs includes any lateral elasticity of the stub pedestals. Local pedestal vertical spring stiffness accounts for floor elasticity and for local rack elasticity just above the pedestal.
- i. Rattling of fuel assemblies inside the storage locations causes the gap between fuel assemblies and cell wall to change from a maximum of twice the nominal gap to a theoretical zero gap. Fluid coupling coefficients are based on the nominal gap in order to provide a measure of fluid resistance to gap closure.
- j. Sloshing is found to be negligible at the top of the rack and is, therefore, neglected in the analysis of the rack.

6.4.3.2 Element Details

The dynamic model of a single rack is shown in Figure 6.4.1. The figure shows many of the characteristics of the model including the fuel to rack gap springs, the rack and fuel bundle elements and the gapped and friction springs at the base that are linked with rigid members.

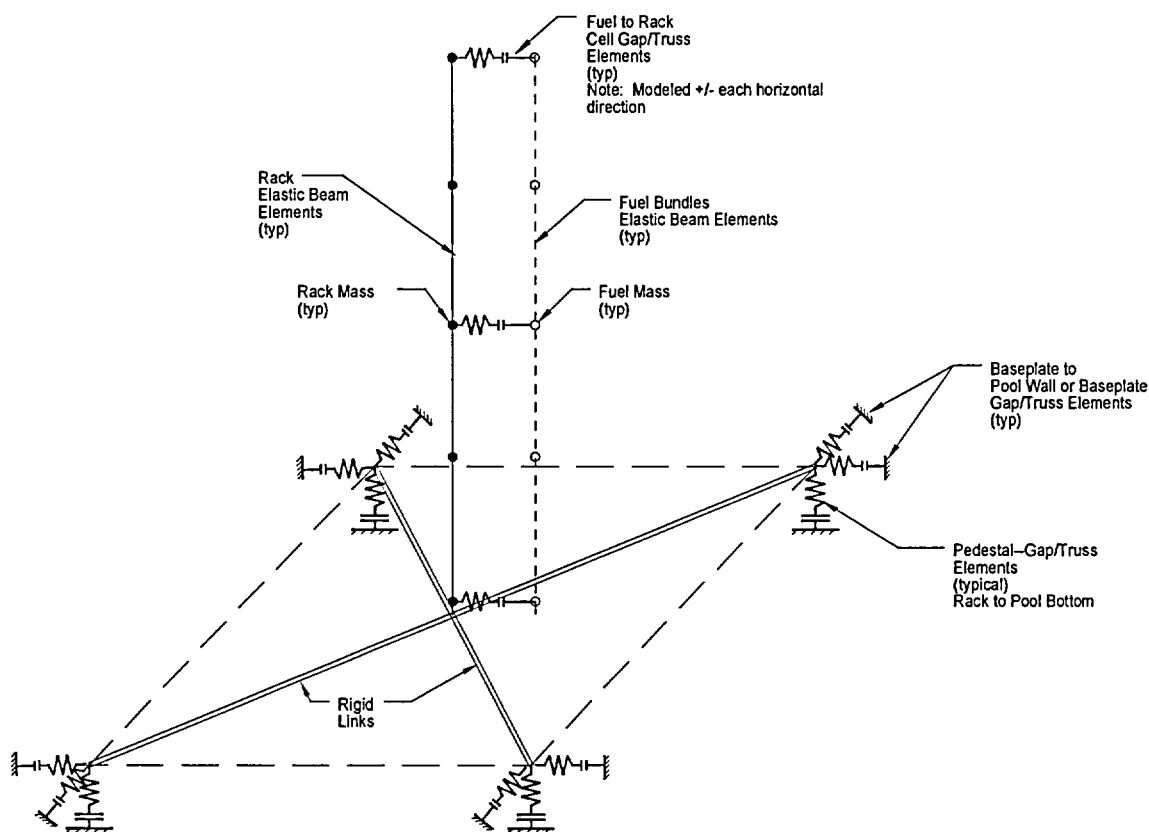


Figure 6.4.1 – Schematic of the Single Rack Dynamic Model

6.4.3.3 Hydrodynamic Coupling Modeling (Single and Multi-Body Coupling)

The hydrodynamic coupling between any two masses is described as “adding” force due to relative motion of the two masses in the X direction. The formulation for this added force is given in Ref. [6.4.1] and is summarized using the following mass matrix formulation:

$$\begin{bmatrix} F_{x1} \\ F_{x2} \end{bmatrix} = \begin{bmatrix} M_1 + M_2 + M_H & -(M_1 + M_H) \\ -(M_1 + M_H) & M_H \end{bmatrix} \begin{bmatrix} \ddot{X}_1 \\ \ddot{X}_2 \end{bmatrix}$$

where,

- F_{x1} - adding force acted on Mass 1
- F_{x2} - adding force acted on Mass 2 (Mass 2 is assumed contained inside Mass 1)
- M_1 - water mass enclosed by Mass 1

- M_2 - displaced water mass by Mass 2
- M_H - hydrodynamic mass
- \ddot{X}_1 - absolute acceleration of Mass 1
- \ddot{X}_2 - absolute acceleration of Mass 2

Therefore, the mass matrix for adding the hydrodynamic coupling force between any two masses is included in the solution process by adding the water masses M_1 , M_2 , and the hydrodynamic mass M_H in each direction to the SOLVIA structural model.

As shown in the above formulation, the motion of one body affects the force field on another. This force field is a function of inter-body gap and can be large when the gaps are small. The lateral motion of a fuel assembly inside a storage location encounters this effect. The rack analysis contains inertial fluid coupling terms, which model the effect of fluid in the gaps between adjacent racks.

Rack-to-rack gap elements have initial gaps set to the entire physical gap between the racks or between outermost racks and the adjacent pool walls.

6.4.3.4 Stiffness Element

There are three element types used in the SOLVIA rack module models. The first element type is linear elastic beam elements used to represent the beam-like behavior of the integrated rack cell matrix. The second element type is the linear friction springs used to develop the forces between the rack pedestals and the supporting floor. The third element type is non-linear gap elements, which model gap closures and impact loadings between fuel assemblies and the storage cell inner walls and racks.

The gap elements modeling impacts between fuel assemblies and racks have local stiffness K_i . Support pedestal spring rates K_s are modeled by gap elements. Local behavior of the pedestal on the concrete floor is included in K_s . The type 2 friction elements are included as K_f . The beam elements for the rack and fuel model the combined stiffness of these components to the racks.

Friction at the support to pool floor interface is modeled by the linear friction springs with stiffness K_f up to the limiting lateral load μN , where N is the current compression load at the interface between support and liner. At every time-step during time history analysis, the current value of N (either zero, if the pedestal has lifted off the floor, or a restraining force) is computed.

The modeling of the effective compression stiffness with the gap element of stiffness K_s includes the pedestal stiffness and local stiffness of the underlying pool slab.

6.4.3.5 Poison Insert Modeling

The poison insert assembly consists of two Metamic panels sheathed in a stainless steel framework which is expanded into the flux trap by a wedge mechanism. The wedges are located at the top, mid-section, and near the bottom of the poison insert assembly. As discussed in Section 6.3.3 the poison insert contribution to stiffness and mass is modeled with the rack beam elements.

6.4.3.6 Friction Modeling Between Rack Supports and Pool Floor

As discussed in 6.3.2.2 simulations are performed with friction coefficients of 0.2, 0.5 and 0.8 in order to bound the range of realistic results for the earthquake event.

6.5 Load Combinations and Load Development

6.5.1 Loads and Load Combinations

The applicable loads and load combinations to be considered in the seismic analysis of rack modules are taken from the OT Position [6.1.2] and are included in Table 6.5.1 below: The acceptance criteria is defined in Subsection NF of the ASME Code [6.5.1].

Table 6.5.1 Load Combinations for the SFP Rack Analysis	
Loading Combination ⁽¹⁾	Acceptance Limit
$D + L$ $D + L + E$	Normal Limits of NF3231.1a ⁽²⁾ , Ref. [6.5.1]
$D + L + T_o$ $D + L + T_o + E$ $D + L + T_a + E$	Lesser of $2 S_y$ or $S_u - \text{Stress Range}^{(1)}$
$D + L + T_a + E'$	Faulted Condition Limits of NF 3231.1c ⁽³⁾ , Ref. [6.5.1]

Notes:

- 1) The thermal loadings have been addressed in detail in the Ref. [6.3.1] calculation and shown to not control the structural evaluations of the racks. Since the normal acceptance limits for the load condition $D + L + E$ is less than the stress range limit, the loading combinations with the stress range limits are not applicable. There is one detail in the design that has changed since the Ref. [6.3.1] calculation. The wedge block design in the Region 3 racks will expand when subjected to temperature. However, this will not cause a lateral load on the flux trap wall. The flux trap wall is composed of the same material as the wedge block and therefore it will expand the same amount and there will be no restraint of the thermal expansion. Therefore, loadings from thermal expansion were not evaluated further.

Stevenson & Associates Report 03Q3428-01

- 2) The design basis is ASME Subsection NF, 1979 through the Winter 1980 Addendum. The rack is evaluated to these code requirements. The new inserts are evaluated to ASME 1998 NF requirements. It is noted that there is no significant difference between these code versions for this application.
- 3) Faulted conditions in the ASME code are defined as Service Level D condition [6.5.1]. NF3231.1c ultimately references Appendix F for this evaluation.

Where:

D = Dead weight-induced loads (including fuel assembly and poison insert weights)

L = Live Load (not applicable for the fuel rack, since there are no moving objects in the rack load path)

E = Operating Basis Earthquake (OBE), including the effects of impacts occurring during the earthquake event.

E' = Safe Shutdown Earthquake (DBE), including the effects of impacts occurring during the earthquake event.

T_o = Differential temperature induced loads (normal operating or shutdown condition based on the most critical transient or steady state condition)

T_a = Differential temperature induced loads (the highest temperature associated with the postulated abnormal design conditions).

As discussed in note 1 above, temperature loadings have been evaluated previously and were not explicitly evaluated, except for their limited effect on member properties. Once temperature is eliminated the two basic governing load combinations evaluated are as follows:

$D + L + E$ (Acceptance Limit Normal Limits of NF3231.1a, Ref. [6.5.1])

$D + L + E'$ (Acceptance Limit is the Faulted Condition Limits, Appendix F, Ref. [6.5.1])

To ease the analysis, the elastic modulus at 150° F was used for both the OBE and DBE dynamic analyses, which results in the best estimate global forces and displacement. The allowable stresses calculated in Subsection 6.7.3 use the yield and ultimate strength properties at 250° F, the highest temperature which results in the lowest allowable stress values. As discussed in OT Position [6.1.2], "for impact loading the ductility ratios utilized to absorb kinetic energy in the tensile, flexural, compressive, and shearing modes should be quantified." Maximum impact loads and therefore maximum ductility ratios will be derived from the DBE event, also ductility ratios are applicable only for faulted condition limits. Therefore, impact loading was only evaluated for the DBE load case. In addition the impact acceptance criteria includes a provision that insures that the

consequent impact loads on the fuel assembly does not lead to damage of the fuel in accordance with the OT Position [6.1.2].

6.5.2 Synthetic Earthquake Time Histories OBE and DBE

The synthetic time-histories in three orthogonal directions (N-S, E-W, and vertical) are generated in accordance with the provisions of SRP [6.1.1], Section 3.7.1. In order to prepare an acceptable set of acceleration time-histories, Stevenson and Associates' commercial code THSPEC [6.5.1] is utilized. It is noted that program THSPEC is a derivative of Program SIMQKE, developed at MIT.

The response spectrum and the power spectral density (PSD) corresponding to the generated acceleration time-history is to envelope their target (design basis) spectrum and PSD with only finite enveloping infractions. The target floor response spectra were developed by interpolating the 2% damped horizontal OBE spectra between 354' and 372' to obtain a spectra at 362'. The vertical OBE spectra at all elevations in the building were used for the vertical response spectra target. It is noted that time history acceleration is independent of damping level, however, due to smoothing and enveloping when developing design spectra, the time history may not envelop all response spectra at a given location developed with different damping coefficients. It is reasonable to use a 2% damped target since this is the damping used in the analysis of welded steel structures. The DBE horizontal design time histories were developed by simply multiplying the OBE time histories by 1.8 and the OBE vertical time history by 2.0 in accordance with APL-C-502 [6.1.4]. The time-histories used for the rack analyses were generated to satisfy the enveloping criterion for the synthetic time-histories in Section 3.7.1 of the SRP [6.1.1]. The seismic files also satisfy the requirements of statistical independence required by SRP 3.7.1 [6.1.1]. The absolute value of correlation function of the three time-histories relative to one another were calculated to be 0.176, 0.167 and 0.142 respectively, which are less than 0.30 (the statistical independence criterion) indicating that the three data sets are statistically independent.

6.5.3 Impact Load Consideration and Combination with other Loads

The impact loading effect on the global rack assemblies is implicitly included by the modeling and dynamic simulations. As described in the modeling, impacts are considered as the gap elements open and close during the analysis.

6.6 Summary of Analyses Perform

6.6.1 Single Rack Analysis

As previously discussed in Section 6.4.1, single rack models were developed for each module type in order to use them as building blocks for the WPMR analysis. In addition the single rack models are employed to study the effect of top loading the rack with miscellaneous equipment. The top loaded rack simulation is performed using the 0.8 coefficient of friction, DBE load case to produce the maximum overturning moment. A

2,000 lbf mass, with three translational degrees-of-freedom, is rigidly attached to the rack 24" above the top of the cell structure. The analysis results, with and without the weight, are studied. It is noted that the results indicate that the additional mass has an insignificant effect on the rack module analysis results.

6.6.2 Whole Pool Multi-Rack (WPMR) Analysis

The multiple rack models use the fluid coupling effects for all racks in the pool. The eight racks are modeled with proper interface fluid gaps and a coefficient of friction at the support interface locations as described in Subsection 6.4.3.6. The response to both DBE and OBE seismic excitation is determined.

6.6.2.1 Parametric Simulations

6.6.2.1.1 Friction Coefficient Variation

The WPMR simulations listed in Table 6.6.1 have been performed to investigate the structural integrity of the racks, including the new poison inserts.

Table 6.6.1				
LIST OF WPMR AND SINGLE RACK SIMULATIONS				
Case	Model	Load Case	COF	Event
1	WPMR	All racks fully loaded	0.5	OBE
2	WPMR	All racks fully loaded	0.2	OBE
3	WPMR	All racks fully loaded	0.8	OBE
4	WPMR	All racks fully loaded	0.5	DBE
5	WPMR	All racks fully loaded	0.2	DBE
6	WPMR	All racks fully loaded	0.8	DBE
7	WPMR	Racks 50% Full ⁽¹⁾	0.5	DBE

COF = Coefficient of Friction

Note 1: The 50% full simulation was performed to determine whether there was a possibility that the racks could exhibit greater displacement when all the cells within the rack are not in use.

6.7 Acceptance Criteria Development

6.7.1 Displacement and Rocking Acceptance Criteria

According to Section 3.8.5 of Ref. [6.1.1], the minimum required safety margins against overturning under the OBE and DBE events are 1.5 and 1.1 respectively. The maximum rotations of the rack (about the two principal axes) are obtained from a post processing of the rack time-history response output. The margin of safety against overturning is given by the ratio of the rotation required to produce incipient tipping in either principal plane to the actual maximum rotation in that plane predicted by the time-history solution.

$$\text{Margin of Safety} = \frac{\theta \text{ required for overturning}}{\theta \text{ predicted}}$$

All ratios for the OBE and DBE events should be greater than 1.5 and 1.1 respectively, to satisfy the regulatory acceptance criteria.

The θ required for overturning is calculated as follows:

The height of the rack is 165" with the center of gravity of the rack to be about the center. The width of the rack between the outside feet is 85.2". The center of the rack has to therefore rock over half the distance between the feet. This angle is defined as:

$$\theta = \sin^{-1} 42.6" \text{ (half the distance between feet)}/82.5" \text{ (distance to the C. G.)} = 31.09^\circ$$

6.7.2 Stress Evaluations – OBE Load Case

The stress limits presented apply to the rack structure and are derived from the ASME Code, Section III, Subsection NF [6.5.1]. Parameters and terminology are in accordance with the ASME Code. Material properties are obtained from the ASME Code Appendices and are listed in Table 6.2.2.

6.7.2.1 Tension Allowable Stress - OBE

Allowable stress in tension on a net section is:

$$F_t = 0.6 S_y$$

$$F_t = 0.6 * 27,500 \text{ psi} = 16,500 \text{ psi}$$

Where S_y = yield stress at temperature, and F_t is equivalent to primary membrane stress.

6.7.2.2 Compression Allowable Stress - OBE

Allowable stress in compression on a net section is:

$$F_a = S_y \left(.47 - \frac{kl}{444r} \right)$$

$$F_a = 27,500 \left(.47 - \frac{kl}{444r} \right)$$

where kl/r for the main rack body is based on the full height and cross section of the honeycomb region and does not exceed 120 for all sections.

l = unsupported length of component

k = length coefficient which gives influence of boundary conditions.

r = radius of gyration of component

6.7.2.3 Shear Allowable Stress - OBE

Allowable stress in shear on a net section is:

$$F_v = 0.4 S_y$$

$$F_v = 0.4 * 27,500 \text{ psi} = 11,000 \text{ psi}$$

6.7.2.4 Bending Allowable Stress - OBE

Maximum allowable bending stress at the outermost fiber of a net section, due to flexure about one plane of symmetry is:

$$F_b = 0.60 S_y \quad (\text{equivalent to primary bending})$$

$$F_b = 0.6 * (27,500 \text{ psi}) = 16,500 \text{ psi}$$

6.7.2.5 Combined Bending and Tension or Compression Allowable Stress - OBE

Combined bending and compression on a net section satisfies:

$$\frac{f_a}{F_a} + \frac{C_{mx} f_{bx}}{D_x F_{bx}} + \frac{C_{my} f_{by}}{D_y F_{by}} < 1$$

where:

f_a = Direct compressive stress in the section

f_{bx} = Maximum bending stress along x-axis

f_{by} = Maximum bending stress along y-axis

C_{mx} = 0.85

$$\begin{aligned}C_{my} &= 0.85 \\D_x &= 1 - (f_a/F'_{ex}) \\D_y &= 1 - (f_a/F'_{ey}) \\F'_{ex,ey} &= (\pi^2 E)/(2.15 (kl/r)^2_{x,y}) \\E &= \text{Young's Modulus}\end{aligned}$$

and subscripts x and y reflect the particular bending plane.

Combined flexure and compression (or tension) on a net section:

$$\frac{f_a}{0.6S_y} + \frac{f_{bx}}{F_{bx}} + \frac{f_{by}}{F_{by}} < 1.0$$

The above requirements are to be met for both direct tension and compression.

6.7.2.6 Bearing Allowable Stress - OBE

Allowable Bearing Stress from Section NF-3226.1 of the ASME Code [6.5.1]:

$$F_b = S_y = 27,500 \text{ psi}$$

6.7.2.7 Weld Allowable Stress or Force (By Analysis and Test) - OBE

Allowable maximum shear stress on the net section of a weld is given by:

$$F_w = 0.3 S_u \text{ (on the weld material) or}$$

$$F_w = 0.4 S_y \text{ (on the base metal material in shear)}$$

$$F_w = 0.6 S_y \text{ (on the base metal material in tension)}$$

where S_u is the weld material ultimate strength at temperature and S_y is the base metal yield strength at temperature. Per Ref. [6.3.1] the weld material used is an E80 electrode with an $S_u = 80$ ksi. For fillet weld legs in contact with base metal, the shear stress on the gross section is limited to $0.4S_y$, where S_y is the base material yield strength at temperature.

Therefore the allowable weld stress is:

$$F_w = 0.3 S_u = .3 * 80 \text{ ksi} = 24 \text{ ksi (on the weld material)}$$

$$F_w = 0.4 S_y = 0.4 * 27,500 \text{ psi} = 11,000 \text{ psi (on the base metal material in shear)}$$

$$F_w = 0.6 S_y = 0.6 * 27,500 \text{ psi} = 16,500 \text{ psi (on the base metal material in tension)}$$

The spot weld allowables were determined by test and were taken as:

$$F_w = T.L. * (S / S_u)$$

Where: *T.L.* is the mean ultimate capacity test results. From Ref. [6.7.1] the mean of the 15 test samples for the spot weld = 680 lb (rounded to the nearest 10 lb)

S = ASME Code Allowable Stress *S* = 17.2 ksi from Ref. 6.5.1 (Note that failure of the test was a base metal failure, therefore, *S*, is the base metal allowable stress.)

S_U = Ultimate Strength from the ASME Code = 68.5 ksi (@250° F) from Ref. [6.5.1]. (Note that failure of the test was a base metal failure, therefore, *S_u*, is the base metal ultimate stress.)

Therefore the allowable spot weld load for the OBE case is:

$$F_w = 680 \text{ lb} * (17.2 / 68.5) = 170 \text{ lb}$$

6.7.3 Stress Evaluations - DBE Load Case

Section F-1334 (ASME Section III, Appendix F [6.6.2]) states that limits for the Level D condition (the stress limits that are applicable to faulted conditions) are the smaller of 2 or $1.167S_u/S_y$ times the corresponding limits for the Level A condition. Examination of material properties for Type 304 stainless steel demonstrates that two times the Level A allowable stress from Service Limit A controls.

6.7.3.1 Tension Allowable Stress - DBE

Allowable stress in tension on a net section is:

$$F_t = 2.0 * 0.6 * 23,750 \text{ psi} = 28,500 \text{ psi}$$

6.7.3.2 Compression Allowable Stress - DBE

Axial Compression Loads are limited to 2/3 of the calculated buckling load or no greater than the allowable tension load:

$$F_a = 0.667 * F_e < 28,500 \text{ psi}$$

Where: F_e is the Euler Buckling Load

6.7.3.3 Shear Allowable Stress - DBE

Stresses in shear shall not exceed the lesser of $0.72S_y$ or $0.42S_u$. In the case of the Austenitic Stainless material used here, $0.72S_y$ governs.

Allowable stress in shear on a net section is:

$$F_v = 0.72 * 23,750 \text{ psi} = 17,100 \text{ psi}$$

6.7.3.4 Bending Allowable Stress - DBE

Maximum allowable bending stress at the outermost fiber of a net section due to flexure about one plane of symmetry is:

$$F_b = 2.0 * 0.6 * (23,750 \text{ psi}) = 28,500 \text{ psi}$$

6.7.3.5 Combined Bending and Tension or Compression Allowable Stress - DBE

Combined bending and compression on a net section satisfies:

$$\frac{f_a}{0.667 * F_e} + \frac{C_{mx} f_{bx}}{2.0 * D_x F_{bx}} + \frac{C_{my} f_{by}}{2.0 * D_y F_{by}} < 1$$

Where all of the terms have been defined in Subsection 6.7.2.5.

Combined flexure and compression (or tension) on a net section:

$$\frac{f_a}{0.667 * F_e} + \frac{f_{bx}}{2.0 * F_{bx}} + \frac{f_{by}}{2.0 * F_{by}} < 1.0$$

Where $0.667 * F_e$ is limited to the tension allowable of 28,500 psi. The above requirements are to be met for both direct tension and compression.

6.7.3.6 Bearing Allowable Stress - DBE

Per Section F-1334.10, Bearing Stress need not be evaluated for loads with Limit D Service Limits are specified.

6.7.3.7 Weld Allowable Stress and Force (By Test) - DBE

For welds, the allowable maximum weld stress is not specified in Appendix F of the ASME Code. An appropriate limit for weld throat stress is conservatively set here as:

$$F_w = 0.3 S_u \text{ x factor (on the weld material)}$$

$$F_w = 0.4 S_y \text{ x factor (on the base metal in shear)}$$

$$F_w = 0.6 S_y \text{ x factor (on the base metal in tension)}$$

where: factor = (Level D shear stress limit) / (Level A shear stress limit) = 17,100/11,000 = 1.55

and S_u and S_y were defined in Subsection 6.7.2.7

Therefore the allowable weld stress is:

$$F_w = 0.3 S_u \text{ x factor} = 1.55 * 0.3 * 80 \text{ ksi} = 37.2 \text{ ksi (weld material)}$$

Stevenson & Associates Report 03Q3428-01

$$F_w = 0.4 S_y \times \text{factor} = 1.55 * 0.4 * 23,750 \text{ psi} = 14,725 \text{ psi (base metal in shear)}$$

$$F_w = 0.6 S_y \times \text{factor} = 1.55 * 0.6 * 23,750 \text{ psi} = 22,088 \text{ psi (base metal in tension)}$$

The spot weld allowables were determined by test from F-13332.7 of Appendix F [6.5.1] and were taken as:

$$F_w = 0.7 * T.L. * (S_U / S_U^*)$$

Where: $T.L.$ and S_U were defined previously in Subsection 6.7.2.7 and S_U^* is the ultimate strength at the testing temperature. Therefore, the ratio S_U / S_U^* is essentially 1.0. Using the Ref. [6.7.1] mean test results of 680 lb the allowable spot weld load for the DBE case is:

$$F_w = 680 \text{ lb} * 0.7 = 475 \text{ lb}$$

6.7.3.8 Impact Acceptance Criteria - DBE

Impact allowable stress will be calculated in accordance with Appendix F of the ASME Code [6.5.1], Section F1341.2 for Plastic Analysis.

In accordance with Section F-1341.2 the general Primary Membrane Stress;

$$P_m < 0.7S_u = 0.7 * 68,500 \text{ psi} = 47,950 \text{ psi}$$

the maximum Primary Stress (including bending from the impact);

$$P_m < 0.9S_u = 0.9 * 68,500 \text{ psi} = 61,650 \text{ psi}$$

6.8 Analysis Results and Comparison to Acceptance Criteria

6.8.1 Time-History Simulation Results

The results from the analyses are contained in the raw data output files. However, due to the huge quantity of output data, a post-processor is used to scan for worst case conditions. Further reduction in this bulk of information is provided in this section by extracting the worst case values from the parameters of interest; namely displacements, support pedestal forces, impact loads, and stress factors. Table 6.8.1 and 6.8.2 below summarize the overall global response of the various Single Rack and WPMR DBE and OBE Analyses respectively.

Stevenson & Associates Report 03Q3428-01

Table 6.8.1 Result Summary – Load Case = DBE						
Rack Global Forces	Single Rack Analysis			Full Pool Analysis		
	F.Coeff=0.2	F.Coeff=0.5	F.Coeff=0.8	F.Coeff=0.2	F.Coeff=0.5	F.Coeff=0.8
Base S _{hx} (lb)	1.43x10 ⁵	1.47x10 ⁵	1.99x10 ⁵	7.804x10 ⁴	1.315x10 ⁵	1.816x10 ⁵
Base S _{hy} (lb)	7.72x10 ⁴	1.37x10 ⁵	2.26x10 ⁵	7.307x10 ⁴	1.84x10 ⁵	2.06x10 ⁵
Axial F (lb)	-4.17x10 ⁴	-4.163x10 ⁴	-4.16x10 ⁴	-4.17x10 ⁴	-4.16x10 ⁴	-4.161x10 ⁴
Base M _{xx} (lb-in)	8.39x10 ⁶	1.715x10 ⁷	2.65x10 ⁷	8.77x10 ⁶	1.913x10 ⁷	2.303x10 ⁷
Base M _{yy} (lb-in)	1.36x10 ⁷	1.77x10 ⁷	2.47x10 ⁷	8.20x10 ⁶	1.386x10 ⁷	1.893x10 ⁷
Base D _x (in.)	2.88	1.274	0.479	1.464	0.2097	0.09895
Base D _y (in.)	4.45	1.236	0.492	3.20	0.6868	0.2437
Top D _x (in.)	2.904	1.299	0.505	1.469	0.2243	0.132
Top D _y (in.)	4.567	1.238	0.520	3.201	0.705	0.2799
Base Acc _x (in./s ²)	226.2	241.4	176.87	280.96	396.3	212.93
Base Acc _y (in./s ²)	123.4	215.8	210.70	175.20	388.5	406.45
Top Acc _x (in./s ²)	258.0	222.9	252.76	341.93	460.78	657.34
Top Acc _y (in./s ²)	146.8	185.54	316.98	190.75	283.3	324.05
Max. Fuel Impact (lb)	1.50x10 ⁵	1.437x10 ⁵	1.914x10 ⁵	1.074x10 ⁵	1.72x10 ⁵	1.903x10 ⁵
Foot -1 (lb)	-1.03x10 ⁵	-1.538x10 ⁵	-2.247x10 ⁵	-1.044x10 ⁵	-1.52x10 ⁵	-1.87x10 ⁵
Foot-2 (lb)	-9.66x10 ⁴	-1.55x10 ⁵	-2.135x10 ⁵	-1.035x10 ⁵	-1.408x10 ⁵	-1.96x10 ⁵
Foot-3 (lb)	-1.08x10 ⁵	-1.63x10 ⁵	-1.88x10 ⁵	-9.958x10 ⁴	-1.47x10 ⁵	-1.717x10 ⁵
Foot-4 (lb)	-1.22x10 ⁵	-1.53x10 ⁵	-2.13x10 ⁵	-9.690x10 ⁴	-1.56x10 ⁵	-2.07x10 ⁵

Note: Results are for the 12x11 rack (group 3)

Stevenson & Associates Report 03Q3428-01

Table 6.8.2 Result Summary – Load Case = OBE						
Rack Global Forces	Single Rack Analysis			Full Pool Analysis		
	F.Coeff=0.2	F.Coeff=0.5	F.Coeff=0.8	F.Coeff=0.2	F.Coeff=0.5	F.Coeff=0.8
Base S _{hx} (lb)	6.20x10 ⁴	1.25x10 ⁵	1.849x10 ⁵	5.56x10 ⁴	1.00x10 ⁵	1.51x10 ⁵
Base S _{hy} (lb)	5.45x10 ⁴	1.28x10 ⁵	1.79x10 ⁵	7.72x10 ⁴	1.25x10 ⁵	1.70x10 ⁵
Axial F (lb)	-3.909x10 ⁴	-3.907x10 ⁴				
Base M _{xx} (lb-in)	6.357x10 ⁶	1.60x10 ⁷	2.30x10 ⁷	8.27x10 ⁶	1.43x10 ⁷	1.97x10 ⁷
Base M _{yy} (lb-in)	7.46x10 ⁶	1.57x10 ⁷	2.23x10 ⁷	6.93x10 ⁶	1.11x10 ⁷	1.53x10 ⁷
Base D _x (in.)	1.113	0.168	0.0473	0.266	0.037	0.0055
Base D _y (in.)	1.446	0.185	0.0473	0.714	0.0708	0.0151
Top D _x (in.)	1.118	0.178	0.0806	0.272	0.0517	0.0321
Top D _y (in.)	1.452	0.203	0.0748	0.7144	0.0935	0.0566
Base Acc _x (in./s ²)	138.66	123.27	147.84	200.1	71.15	50.17
Base Acc _y (in./s ²)	96.57	114.01	144.14	135.50	125.81	58.55
Top Acc _x (in./s ²)	98.83	160.93	263.19	255.48	373.53	390.60
Top Acc _y (in./s ²)	82.10	167.40	190.67	133.16	260.37	231.69
Max. Fuel Impact (lb)	7.52x10 ⁴	1.246x10 ⁵	1.264x10 ⁵	1.16x10 ⁵	1.18x10 ⁵	1.176x10 ⁵
Foot -1 (lb)	-9.68x10 ⁴	-1.48x10 ⁵	-1.98x10 ⁵	-9.31x10 ⁴	-1.28x10 ⁵	-1.51x10 ⁵
Foot-2 (lb)	-9.63x10 ⁴	-1.43x10 ⁵	-1.99x10 ⁵	-9.38x10 ⁴	-1.32x10 ⁵	-1.61x10 ⁵
Foot-3 (lb)	-9.18x10 ⁴	-1.38x10 ⁵	-2.01x10 ⁵	-8.97x10 ⁴	-1.25x10 ⁵	-1.61x10 ⁵
Foot-4 (lb)	-9.78x10 ⁴	-1.46x10 ⁵	-1.95x10 ⁵	-9.31x10 ⁴	-1.41x10 ⁵	-1.71x10 ⁵

Note:

Results are for the 12x11 rack (group 3)

Stevenson & Associates Report 03Q3428-01

Output results from SOLVIA for the controlling case for maximum fuel-cell impact are shown in Figures 6.8.1 and 6.8.2 for the single rack model and Figure 6.8.3 and 6.8.4 for the WPMR model.

The Subsections that follow summarize additional analyses performed to develop and evaluate structural member stresses, which are not determined by the post processor.

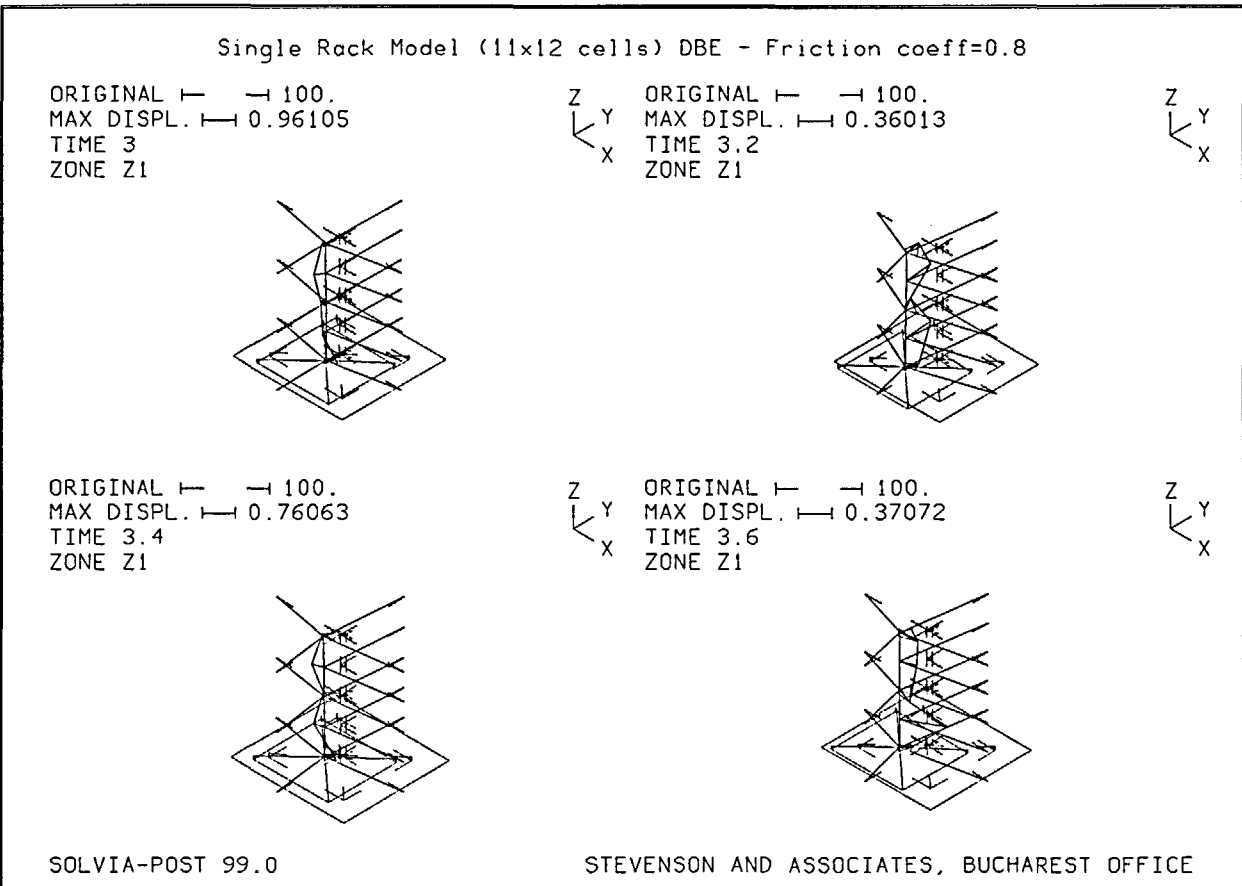


Figure 6.8.1 - Maximum Displacement Plots (in.), Single Rack Model, $\mu = 0.8$

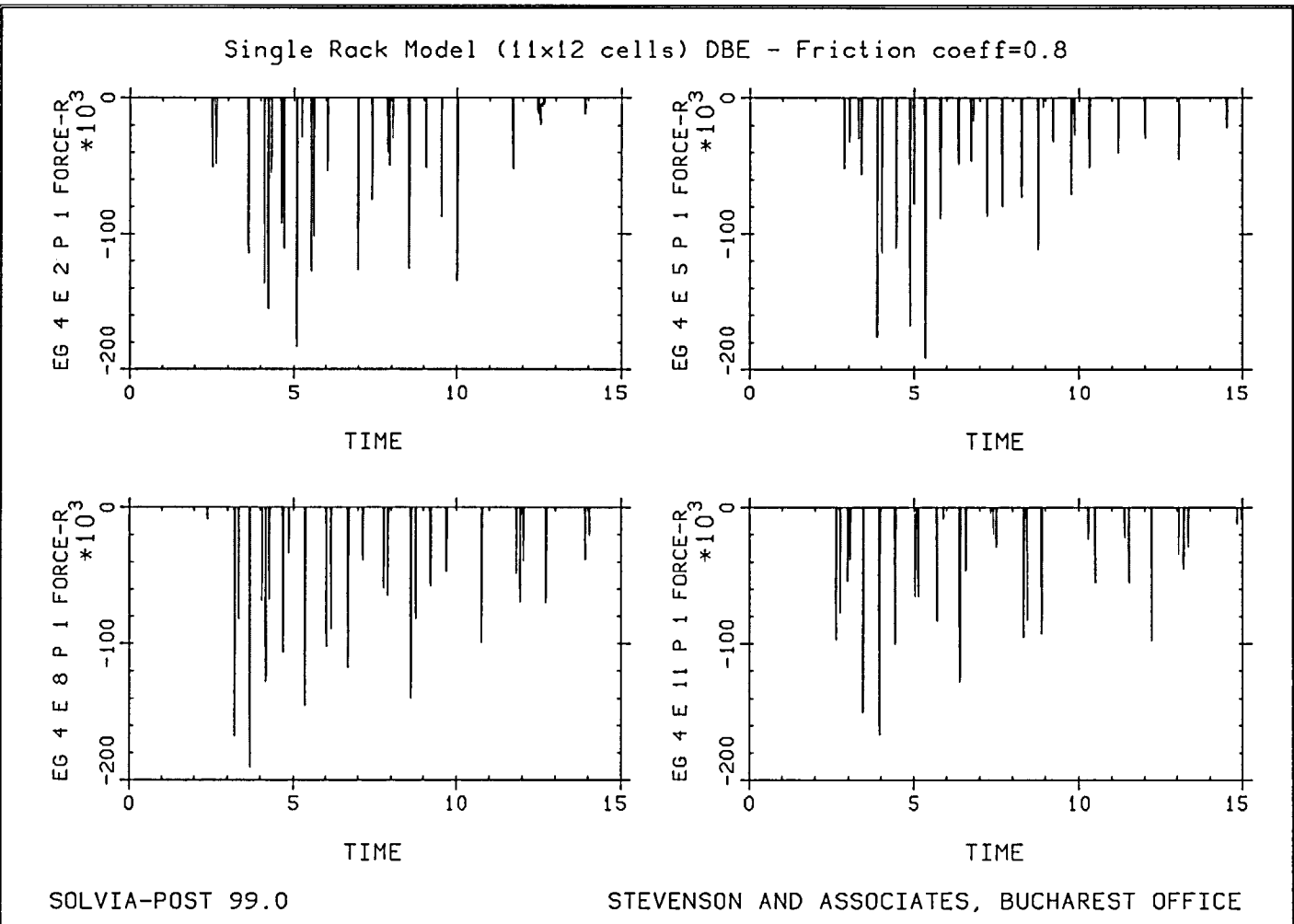


Figure 6.8.2 - Cell Impact Force Plots (lb), Single Rack Model, $\mu = 0.8$

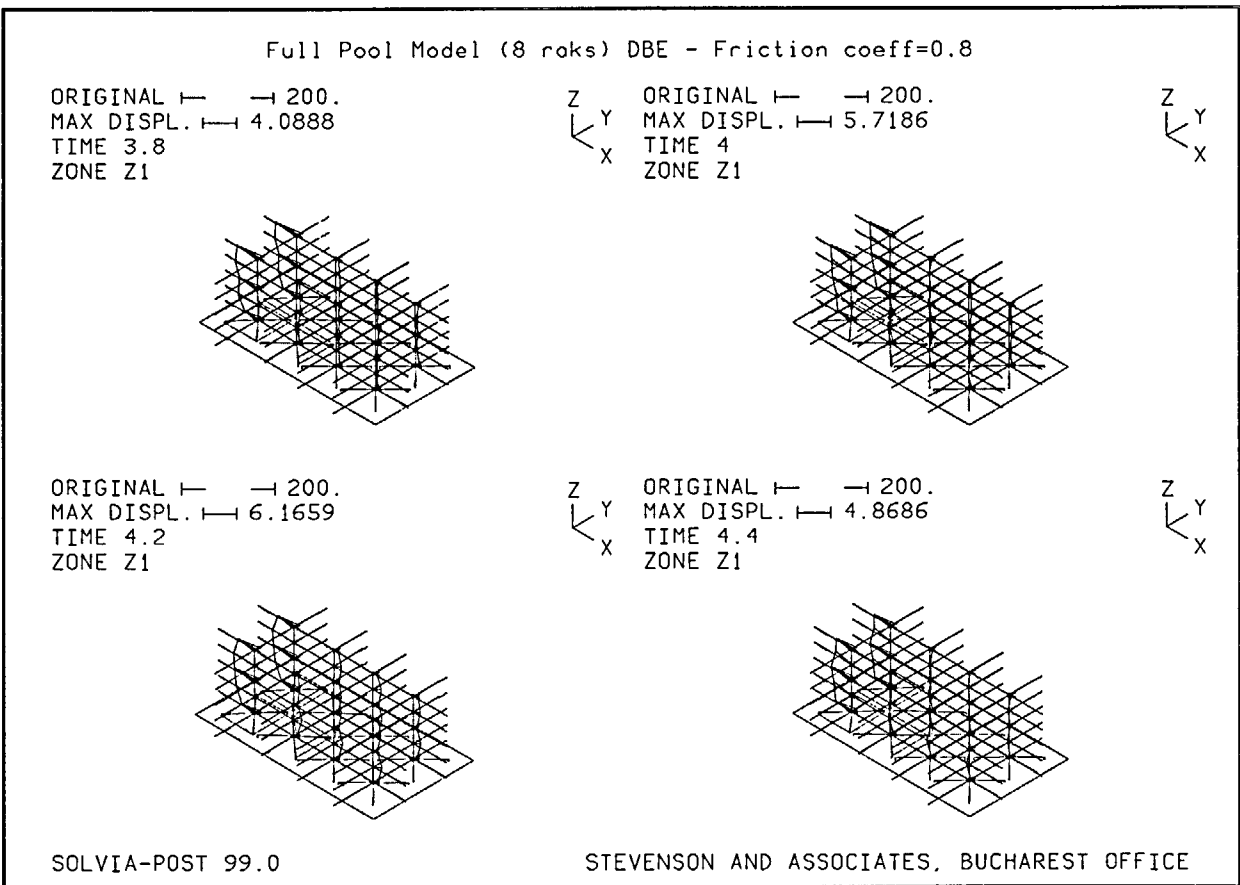


Figure 6.8.3 - Maximum Displacement Plots (in.), WPMR Model, $\mu = 0.8$

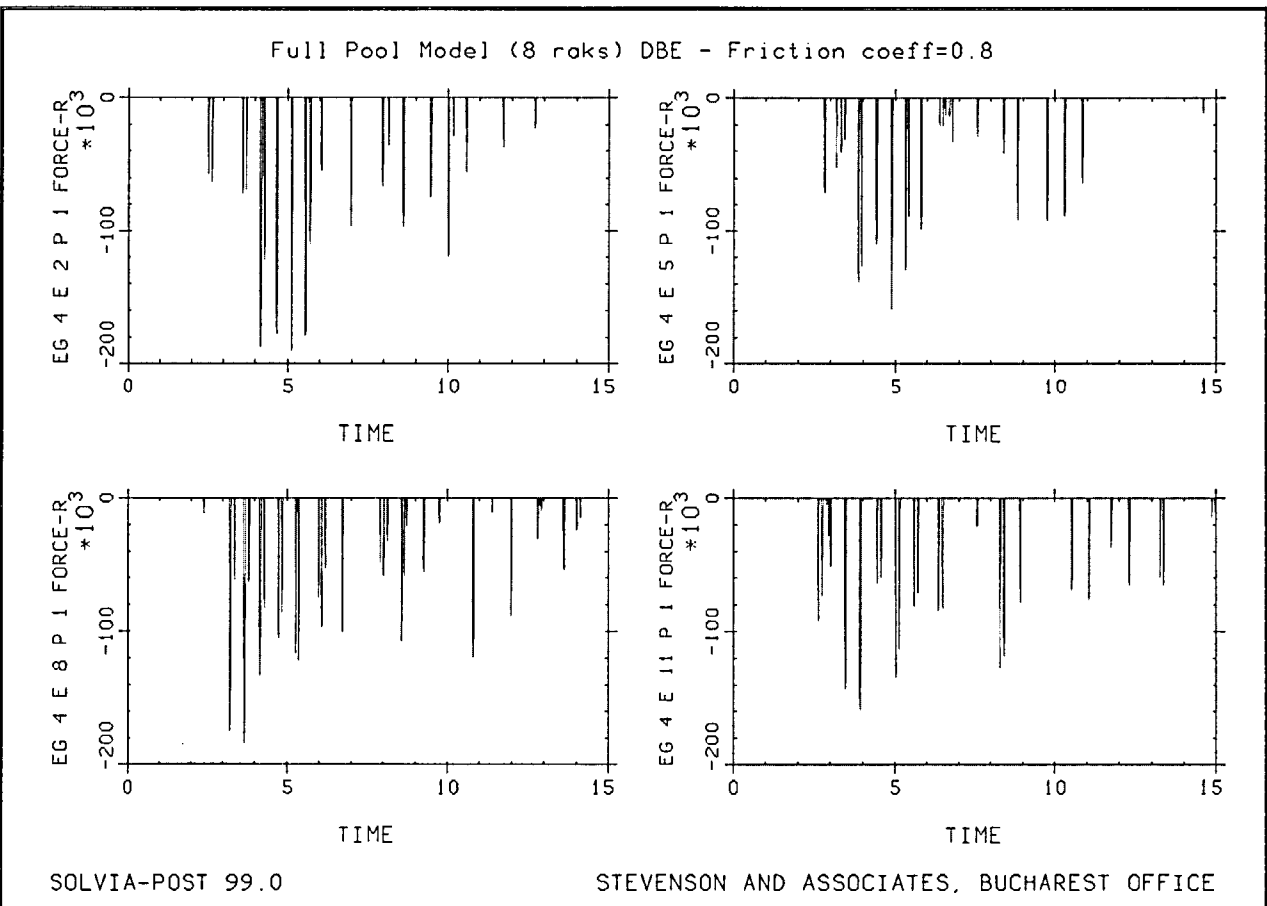


Figure 6.8.4 - Cell Impact Force Plots (lb), WPMR Model, $\mu = 0.8$

6.8.2 Maximum Rack Displacements and Rocking

The maximum rack displacements are obtained from the time-histories of the motion of the upper and lower four corners of each rack in each of the simulations. The maximum displacements in either direction reported from the WPMR analyses are 3.2" for the DBE event and 0.71" for the OBE event. The maximum displacements in either direction reported from the single rack analysis are 4.6". The rack height is 165" from the floor to the top of the rack. Making the conservative assumption that the displacement of the rack at the base is 0" (somewhat unrealistically conservative since the majority of this displacement is from sliding) results in the following:

The rocking angle of the rack for the OBE displacement is:

$$\Theta \text{ (predicted)} = \sin^{-1} (0.71" / 165") = 0.25^\circ$$

$$\text{Margin of Safety} = \frac{\theta \text{ required for overturning}}{\theta \text{ predicted}} =$$

31.09° (calculated in Subsection 6.7.1)/0.25° = 124.4 >> 1.5 (from Subsection 6.7.1) OK

The rocking angle of the rack for the DBE small displacement is:

$$\Theta \text{ (predicted)} = \sin^{-1} 4.6" / 165" = 1.60^\circ$$

$$\text{Margin of Safety} = \frac{\theta \text{ required for overturning}}{\theta \text{ predicted}} =$$

31.09° (calculated in Subsection 6.7.1)/1.60° = 19.46 >> 1.1 (from Subsection 6.7.1) OK

6.8.3 Pedestal Evaluation

6.8.3.1 Maximum Pedestal Vertical Forces

The maximum vertical pedestal force obtained in the WPMR simulations was 40,200 lb for the OBE Condition. The maximum vertical pedestal force obtained in the WPMR simulations was 44,940 lb for the DBE Condition.

6.8.3.2 Maximum Pedestal Horizontal Forces (From Friction)

The maximum interface shear force value bounding all pedestals in the WPMR simulations for the OBE in the X direction is 13,207 lb and in the Y direction 12,786 lb. The maximum interface shear force value bounding all pedestals in the WPMR simulations for the DBE in the X direction is 14,214 lb and in the Y direction 16,143 lb.

6.8.3.3 Pedestal and Pedestal Connection Structural Evaluation

The time-history results from the analyses provide the pedestal normal and lateral interface forces, which may be converted to the limiting bending moment and shear force at the bottom baseplate-pedestal interface. Maximum values are determined for every pedestal in the array of racks. With this information available, the structural integrity of the pedestal was assessed. The net section maximum bending moments and shear forces can also be determined at the bottom baseplate-rack cellular structure interface for each spent fuel rack in the pool. Using these forces and moments, the maximum stress on the worst case pedestal was calculated.

For the OBE condition the maximum stress for axial and bending loads calculated for the pedestal supports was:

9,466 psi < 16,500 psi allowable (Subsection 6.7.2.1, 6.7.2.4 and 6.7.2.5) OK

Note that for this interaction, the interaction equation $\frac{f_a}{0.6S_y} + \frac{f_{bx}}{F_{bx}} + \frac{f_{by}}{F_{by}} < 1.0$ controls the combined bending and axial load interaction and the $0.6 S_y = F_b = 16,500$ psi

For the DBE condition the maximum stress for axial and bending loads calculated for the pedestal supports was:

10,848 psi < 28,500 psi allowable (Subsection 6.7.3.1, 6.7.3.4 and 6.7.3.5) OK

Note that for this interaction, the interaction equation $\frac{f_a}{0.667 * F_e} + \frac{f_{bx}}{2.0 * F_{bx}} + \frac{f_{by}}{2.0 * F_{by}} < 1.0$ controls since $0.667 * F_e$ is limited to 28,500 psi = $2.0 * F_b$.

For the OBE condition the maximum bearing stress calculated for the pedestal supports was:

8,388 psi < 27,500 psi allowable (Subsection 6.7.2.6) OK

The DBE condition does not have to be evaluated for bearing as discussed in Subsection 6.7.3.6.

For the OBE condition the maximum shear stress in the pedestal support threads was:

8,232 psi < 11,000 psi allowable (Subsection 6.7.2.3) OK

For the DBE condition the maximum shear stress in the pedestal support threads was:

9,417 psi < 17,100 psi allowable (Subsection 6.7.3.3) OK

6.8.4 Rack Structural Evaluation

6.8.4.1 Rack Member Evaluations

The time-history results from the analyses provide the maximum internal section forces and moments which may be converted to the limiting stresses within the rack. The limiting maximum combined rack stress interaction coefficient for axial and bending stresses for the OBE = 0.694 < 1.0 allowable and for the DBE = 0.452 < 1.0 allowable. These evaluations include the worst case rack members in the rack.

6.8.4.2 Rack Connection Evaluations

Weld locations subjected to significant seismic loading are at the bottom of the rack at the baseplate-to-cell connection, at the top of the pedestal support at the baseplate connection, and at cell-to-cell connections. Bounding values of resultant loads are used to qualify the connections.

a. Baseplate-to-Rack Cell Welds

Weld stresses are produced through the analysis of the rack cell welds for the maximum loads on the sections. In the case of the baseplate to the rack cell the base metal section controlled the evaluation.

The highest predicted cell to baseplate base metal stress in tension for the OBE is calculated as:

$$14,240 \text{ psi} < 16,500 \text{ psi allowable (Subsection 6.7.2.7) OK}$$

The highest predicted cell to baseplate base metal stress in tension for the DBE is calculated as:

$$16,047 \text{ psi} < 22,088 \text{ psi allowable (Subsection 6.7.3.7) OK}$$

b. Wrapper Plate Welds

The fuel cells are composed of two L-shaped formed sections, placed to form a box section and welded at the opposite corners. The wrapper plates form the flux traps on the outside of each side of the cell box. The wrapper plates are welded to each cell side by 0.03 inch fillet welds, 1.5" long at 8" centers. Alternatively, spot welds could be used with three options on size and spacing. The maximum force in these welds occurs near the base. The limiting shear on these welds was calculated based on comparison to the Ref. [6.3.1] results. Note that for these welds the base metal material in shear governs.

Limiting Shear for OBE 8,847 psi < 11,000 psi allowable (Subsection 6.7.2.7) OK

Limiting Shear for DBE 10,192 psi < 14,725 psi allowable (Subsection 6.7.3.7) OK

c. Cell Seam Welds

The cell seam welds are at opposite corners of each cell and are nominally 0.035" fillet welds that are 4" long at the bottom of the cell and on 8" centers at the top. An optional butt weld of 0.055" is adequate if the 0.035" fillet welds is shown to be adequate. The maximum force on these welds occurs near the base.

The limiting shear on these welds is also calculated based on comparison to the Ref. [6.3.1] results. Note that for these welds the weld material governs.

Max. Shear for OBE is 18,786 psi < 24,000 psi allowable (Subsection 6.7.2.7) OK

Max. Shear for DBE is 21,642 psi < 37,200 psi allowable (Subsection 6.7.3.7) OK

d. Cell-to-Cell Welds

Cell-to-cell connections are by a series of connecting welds along the cell height. The weld stress is calculated based on the cell wall base metal stresses resulting from the maximum shear flow developed between two adjacent cells under OBE and DBE conditions. Note that the contributions from impact loads are included in the maximum shear flow.

The limiting shear on these welds is also calculated based on comparison to the Ref. [6.3.1] results. Note that for these welds the weld material governs.

Max. Shear for OBE is 19,681 psi < 24,000 psi allowable (Subsection 6.7.2.7) OK

Max. Shear for DBE is 22,673 psi < 37,200 psi allowable (Subsection 6.7.3.7) OK

6.8.5 Support Plate Evaluation

The total shear stress on the support plate was calculated for the loads transmitted from the pedestals. The maximum shear stress for OBE loads was calculated to be:

$$f_v = 2534 \text{ psi} < 11,000 \text{ psi allowable (Subsection 6.7.2.3) OK}$$

The maximum shear stress for DBE loads was calculated to be:

$$f_v = 2917 \text{ psi} < 17,100 \text{ psi allowable (Subsection 6.7.3.3) OK}$$

6.8.6 Poison Insert Evaluations

The poison insert assemblies were evaluated for the potential local response of the insert due to seismic excitation. DBE loads and stresses on the structural components of the poison insert assembly were evaluated for loads from the DBE. The Metamic insert has an $S_u = 40.67$ ksi and an $S_y = 33.1$ ksi from Ref. [6.8.5]. The allowable stresses described in this Subsection are consistent with those described in detail in Subsection 6.7.2 but adjusted for these member properties. The loads and stresses for the DBE loads are conservatively compared to OBE allowable stress criteria, and therefore, both OBE and DBE conditions are evaluated.

Stevenson & Associates Report 03Q3428-01

The maximum bending stress for DBE loads in the Metamic panel was calculated to be:

$$f_b = 2,596 \text{ psi} < 0.6 * 33,100 \text{ psi} = 19,860 \text{ psi OK}$$

The enclosure channel is the same SA240, Type 304 material as the rack. The maximum bending stress for DBE loads in the enclosure channel was calculated to be:

$$f_b = 2,989 \text{ psi} < 16,500 \text{ psi allowable (Subsection 6.7.2.1) OK}$$

The shear force loads on the two spot welds were for DBE loads were calculated to be only:

$$4.5 \text{ lb} \ll 312 \text{ lb capacity for the two welds (from Subsection 6.7.2.7) OK}$$

The maximum vertical load for DBE loads on the Metamic panel was calculated to be:

$$F_{\text{axial}} = 14.9 \text{ lb} < 64.9 \text{ lb allowable (calculated based on 2/3 the Euler Buckling load) OK}$$

The maximum vertical load for DBE loads on the enclosure plates was calculated to be:

$$F_{\text{axial}} = 9.2 \text{ lb} < 145.7 \text{ lb allowable (calculated based on 2/3 the Euler Buckling load) OK}$$

6.8.7 Impact Evaluation

6.8.7.1 Local Stress Evaluations Due to Impact Between the Fuel Assembly and Cell Wall

Local cell wall integrity is conservatively estimated from peak impact loads. Plastic analysis is used to obtain the limiting impact load that could lead to gross permanent deformation. As shown in Table 6.8.1, the maximum impact force between the fuel and the rack occurs for the DBE loading for the single rack analysis with a coefficient of friction of 0.8.

The impact force applicable for a single cell is:

$$1.914 \times 10^5 / 132 = 1450 \text{ lb}$$

This load was applied to a two cell finite element model of the cell wall to determine the local stress on the wall. A plastic analysis of the two cell model was analyzed for this load with and without the wedge blocks and considering the wedge blocks located at the point of impact. The maximum primary stress for this case occurs for the case without the wedge blocks with a value of:

$$P_m = 21,411 \text{ psi} < 47,950 \text{ psi allowable (Subsection 6.7.3.8) OK}$$

The plastic analysis performed ensures that the primary membrane plus bending loads are limited to about the yield strength of the material and therefore, the primary membrane plus bending stress limitation is implicitly enforced.

6.8.7.2 Evaluation of the Fuel Assembly

The permissible lateral load on an irradiated spent fuel assembly has been studied by the Lawrence Livermore National Laboratory (LLNL). The LLNL report [6.8.1] states that "...for the most vulnerable fuel assembly, axial buckling varies from 82g's at initial storage to 95g's after 20 years' storage. In a side drop, no yielding is expected below 63g's at initial storage to 74g's after 20 years' [dry] storage."

The maximum fuel-to-storage cell rattling force from the WPMR runs is 1,450 lb calculated above. The weight of a fuel assembly is 1700 lb. By inspection, the impact force from a side drop at 63 g's of the 1700 lb assembly is much greater than the 1450 lb impact load from the analysis and therefore, the fuel assembly is acceptable.

6.8.7.3 Rack to Wall or Rack to Rack Impact Loads

The storage racks do not impact the pool walls or adjacent racks under any simulation. The rack to rack or rack to wall gap elements did not close during the analytical simulations.

6.8.8 Consideration of Miscellaneous Equipment Loads

An additional load of 2000 lbs can temporarily be set on top of the Region 2 racks. It was concluded that the presence of this equipment does not impact the seismic qualification of the racks. Similarly, a 200 lb weight considered to represent testing equipment which may be placed anywhere on the top of any rack has an inconsequential effect on the seismic adequacy of the racks.

6.8.9 Analysis considering Half Full Fuel Racks

An additional analysis was performed for a condition where the Region 3 racks were considered half full. This was run for the DBE Full Pool Analysis for a 0.8 coefficient of friction since this was the controlling case for all full pool analyses with the racks full. When compared to the results for the full rack conditions, this case was found not to control for the racks.

6.8.10 Comparison of Analysis Results to Westinghouse Ref. [6.3.1] Results

The Westinghouse analysis in Ref. [6.3.1] evaluated the racks without the Metamic inserts. The methodology was similar to that used in the Stevenson & Associates evaluation of Ref. [6.1.5]. Table 6.8.3 below presents a comparison of component stresses that were independently calculated. As shown in the table, the results were very similar. This comparison is a further validation of the Stevenson & Associates Ref. [6.1.5] evaluation and that the use of the Westinghouse results for the Wrapper welds, cell seam weld and cell-to-cell weld is justified. Note that the S&A results are generally slightly less than those by Westinghouse. Potential reasons for this include the likelihood of less conservatism in the time history functions used by S&A and more accurate modeling of the fuel assemblies. The higher impact forces obtained by S&A are due in

Stevenson & Associates Report 03Q3428-01

part to the larger impact stiffness used, which considers the addition of the inserts and the potential for impact at the wedge block locations.

Table 6.8.3 – Comparison of the Stress Results for OBE Load Case between Westinghouse [6.3.1] and Stevenson & Associates [6.1.5]				
Component	Stress Type	D + L + E		
		Stress from S&A Analysis (psi)	Stress from Westinghouse Analysis (psi)	% Difference (S&A results as base)
Cell	Axial+Bending	11,316	11,826	4.5%
Cell to Base Plate Welds	Shear	14,240	14,369	0.9%
Support Pad	Axial	9,466	9,654	2.0%
	Shear	2,216	2,544	14.8%
	Bearing	8,388	8,492	1.2%
Threads	Shear	8,232	8,275	0.5%
Support Plate	Shear	2,534	2,951	16.5%

6.9 Conclusions

The overall design objectives of the spent fuel storage pool at ANO Unit 1 have been shown to meet the various Regulatory Guides, the Standard Review Plan, and industry standards. The structural adequacy of the SFP maximum density spent fuel racks at ANO Unit 1 with the new poison inserts have been evaluated using the appropriate regulatory and design standards. Postulated loadings for normal, seismic, and accident conditions at the ANO Unit 1 site were considered in this analysis and evaluation. The design adequacy of the racks and the poison inserts has been confirmed with analyses that were performed in compliance with the USNRC Standard Review Plan [6.1.1], the USNRC Office of Technology Position Paper [6.1.2], Lawrence Livermore Report UCRL52342 [6.1.3] and ANO Specification APL-C-502 [6.1.4]. All applicable displacement and stress acceptance criteria have been met for the racks and the new poison inserts, as summarized for the OBE and DBE in Tables 6.9.1 and 6.9.2 below.

Table 6.9.1 -- Summary of Stress Results for OBE Load Case				
Component	Stress Type	D + L + E		
		Applied Stress (psi)	Allowable Stress (psi)	Stress Interaction
Cell	Axial+Bending	11,421	16,500	0.692
Wrapper Welds	Shear	8,847	11,000	0.804
Cell Seam Welds	Shear	18,786	24,000	0.783
Cell to Cell Welds at Top at Bottom	Shear	12,259	24,000	0.511
	Shear	19,681	24,000	0.820
Cell to Base Plate Welds	Tension	14,240	16,500	0.863
Support Pedestal	Axial	9,466	16,500	0.574
	Shear	2,216	11,000	0.202
	Bearing	8,388	27,500	0.305
Threads	Shear	8,232	11,000	0.748
Support Plate	Axial	352	16,500	0.021
	Shear	2,534	11,000	0.230
Metamic Insert Metamic Panel	Bending	2,622	19,860	0.132
	Axial	15 lb	64.9 lb	0.230
	Spot Welds	Shear Force	2.25 lb	340 lb
Enclosure Channel	Bending	20,072	28,500 (1)	0.704
	Axial	9.2 lb	18.4 lb	0.50

Note: 1) The allowable stress shown for the enclosure channel of the Metamic insert is a DBE allowable stress. The applied stress is limited by the maximum displacement and is the same for the OBE and DBE load case.

Table 6.9.2 -- Summary of Stress Results for DBE Load Case				
Component	Stress Type	D + L + E'		
		Applied Stress (psi)	Allowable Stress (psi)	Stress Interaction
Cell	Axial+Bending	12,880	28,500	0.452
Wrapper Welds	Shear	10,192	17,100	0.596
Cell Seam Welds	Shear	21,642	37,200	0.582
Cell to Cell Welds at Top at Bottom	Shear	14,122	37,200	0.380
	Shear	22,673	37,200	0.609
Cell to Base Plate Welds	Tension	16,047	22,088	0.727
Support Pedestal	Axial	10,848	28,500	0.381
	Shear	2,593	17,100	0.152
	Bearing	9601	N/A	N/A
Threads	Shear	9,417	17,100	0.551
Support Plate	Axial	379	28,500	0.013
	Shear	2,917	17,100	0.171
Impact Loads on Cells With Wedge Blocks Without Wedge Blocks	Membrane	7,514	47,950	0.157
	Tension	21,411	47,950	0.447
Metamic Insert	See OBE--Evaluated for DBE Loads with OBE Allowables			

It is noted that the addition of the inserts to the existing racks has only a slight impact on their dynamic response. The added stiffness of the inserts is small and the mass is extremely small in comparison to the hydrodynamic mass which dominates the response. The region 3 spent fuel racks have been shown to be seismically adequate with the addition of the Metamic poison inserts. Additionally, the poison inserts have been shown adequate for seismic induced loads.

6.10 References

- [6.1.1] USNRC NUREG-0800, Standard Review Plan, June 1987.
- [6.1.2] (USNRC Office of Technology) "OT Position for Review and Acceptance of Spent Fuel Storage and Handling Applications", dated April 14, 1978, and January 18, 1979 amendment thereto.
- [6.1.3] UCRL52342, "Effective Mass and Damping of Submerged Structures", Lawrence Livermore National Laboratory, April 1, 1978.
- [6.1.4] ANO Technical Specification APL-C-502, "Technical Specifications for Earthquake Resistance Design of Structures and/or Components Located in the Auxiliary Building for the Arkansas Nuclear One Unit 1 Power Plant", Rev. 2, 4-22-87.
- [6.1.5] Stevenson & Associates Calculation ANO-ER-02-051, "Seismic Re-qualification of the Arkansas Nuclear One Unit 1 Spent Fuel Racks," Rev. 0, Dec. 23, 2003.
- [6.2.1] Westinghouse Drawing 1-W62A-017(1)-0
- [6.3.1] Calculation 91E-0079-01, Revision 1, "Design Report for Spent Fuel Storage Racks for AP&L Co. 9-20-96 (analysis performed in 1982).
- [6.3.2] Levy, S. and Wilkinson, J.P.D., "The Component Element Method in Dynamics with Application to Earthquake and Vehicle Engineering", McGraw Hill, 1976.
- [6.3.3] Rabinowicz, E., "Friction Coefficients of Water-Lubricated Stainless Steel for a Spent Fuel Rack Facility," Massachusetts Institute of Technology, November 1976.
- [6.4.1] ASCE Standard 4-98, "Seismic Analysis of Safety Related Nuclear Structures and Commentary", American Society of Civil Engineers, Copyright 2000.
- [6.4.2] Stevenson & Associates Report, "Independent Evaluation of Seismic Response of Spent Fuel Storage Racks Currently Being Procured for Salem Nuclear Power Plant", Dec. 1, 1993.
- [6.4.3] NUREG/CR-5912, BNL-NUREG-52335, "Review of the Technical Basis and Verification of Current Analysis Methods Used to Predict Seismic Response of Spent Fuel Storage Racks", Brookhaven National Laboratory, October 1992.
- [6.5.1] ASME Boiler & Pressure Vessel Code, Section III, Subsection NF, 1980, through Winter 1981 Addendum.

Stevenson & Associates Report 03Q3428-01

- [6.5.2] Stevenson and Associates, Program THSPEC – Verification and User’s Manual for Computer Code THSPEC.
- [6.6.2] ASME Boiler & Pressure Vessel Code, Section III, Appendices, 1980, through Winter 1981 Addendum.
- [6.7.1] Stork Herron Testing Labs, Specimen Load Tests, Dec. 18, 2003.
- [6.8.1] Chun, R., Witte, M. and Schwartz, M., “Dynamic Impact Effects on Spent Fuel Assemblies”, UCID-21246, Lawrence Livermore National Laboratory, October 1987.
- [6.8.2] ACI 349-85, Code Requirements for Nuclear Safety Related Concrete Structures, American Concrete Institute, Detroit, Michigan, 1985.
- [6.8.3] ACI 318-95, Building Code Requirements for Structural Concrete, American Concrete Institute, Detroit, Michigan, 1995.
- [6.8.4] Entergy letter to the NRC dated April 2, 2003. “License Amendment Request to Modify the Fuel Assembly Enrichment, the Spent Fuel Pool (SFP) Boron Concentration Technical Specification (TS) 3.7.14, the Loading Restrictions in the SFP in TS 3.7.15, and to Modify the Fuel Storage Design Features in TS 4.3”
- [6.8.5] Entergy letter to Stevenson & Associates – ANO-2003-00144, dated Dec. 8, 2003, Subject: "Spent fuel Pool Inputs Required for the Unit 1 Rack Seismic Analysis."

Attachment 2

To

1CAN120302

Revised Portions of Original Submittal (1CAN040302)

Attachment 4 of 1CAN040302

Section 1.0, Introduction - 4th paragraph

The ANO-1 spent fuel racks consist of individual cells with a square pitch of 10.65 inches, each of which accommodates a single B&W 15x15 fuel assembly or equivalent. The ANO-1 SFP is divided into two regions, designated Region 1 and Region 2. Region 1 racks employ Boraflex as the poison material and are presently qualified to store fresh fuel assemblies with enrichments up to 4.1 weight percent (wt%) ²³⁵U. Region 2 racks are designed with flux-traps and are currently used to store spent fuel assemblies with various initial enrichments that have accumulated certain minimum burn-ups. These racks do not have any poison material. Some of the Region 2 racks will be modified by the insertion of Metamic[®] absorber panels into the flux trap region to create a Region 3. These different regions are depicted in Figure 1-1. These poison inserts will have two borated Aluminum (Metamic[®]) panels as neutron absorbers. Each poison insert panel will be held in the flux trap along the cell wall by a stainless steel frame with a wedge/hook mechanism. The insertion of the Metamic[®] poison panels into the new region, as shown by analyses later in this report, will enable storage of fresh fuel with a maximum enrichment up to 5.0 weight percent (wt%) in the ANO-1 SFP. The Region 3 flux traps will be fitted with lead-ins on the top of the flux traps, which will act to prevent any possible uplifting of the poison panel insert. The lead-in devices will also help guide the fuel assemblies into the storage cells.

Attachment 4 of 1CAN040302

Section 2.0, Spent Fuel Rack Flux Trap Gap Poison Insert Design – Section 2.5, 2nd and 3rd paragraphs

The poison panels will be held together with a frame that is fabricated from SA240-304 stainless steel. A schematic of the arrangement is shown in Figure 2.5.1. Figure 4.3.2 depicts the current Region 2 cell with four flux traps. Each poison insert is composed of two interconnected Metamic rectangular poison panel assemblies. Each Metamic poison panel assembly includes a Metamic poison panel protected and held in place by stainless steel sheathing bands. Full-length sheathing covers the side of the Metamic panel facing the flux trap wall. This will prevent any direct contact between the Metamic panel and the flux trap wall. Additional stainless steel bands connect the two panel assemblies together. The poison insert remains in a closed configuration before installation. The poison insert assembly is designed to open up to fill the flux trap gap by gravity only. The poison insert includes a hook/wedge mechanism. The hook/wedge mechanism maintains the poison insert in an opened configuration once installed in the flux trap and also maintains contact

between the poison insert with the flux trap wall. The poison insert assemblies are designed based on worst-case measured dimensions of the flux trap and maximizing use of the allowable space in each flux trap for criticality safety purposes.



Figure 2.5.1 Schematic of the Poison Insert Mechanism

The lead-in device, which is depicted in Figure 2.5.2, is fabricated from SA240-304 stainless steel. The device is designed to rest on top of the flux trap, and it is secured in place by two slotted plates, which straddle the cell wall at the corners external to the flux trap. The size and shape of the lead-in is such that it will not interfere with the square opening of the cell. The lead-in contains flow holes in the mounting plate to provide an uninterrupted flow path for the water entering at the bottom of the flux trap and exiting at the top of the flux trap. Each poison insert and lead-in device together weighs less than 50 lbs.

Attachment 4 of 1CAN040302
Section 3.0, Material Considerations – Section 3.5, 1st Paragraph

There are no heavy loads involved in the proposed installation of poison inserts. The weight of a single poison insert and a lead-in is less than 50 pounds.

Attachment 5 of 1CAN040302 - 5th paragraph
Evaluation of Spent Fuel Pool Structural Integrity for Increased Loads from Spent Fuel Racks

The recent evaluation of the spent fuel racks by Stevenson & Associates was performed to evaluate the effects on two of the racks for the additional weight of proposed poison inserts to two of the racks. This evaluation included analyses of the racks as described in Sections 3 through 6, and resulted in revised loads imparted from the racks to the pool floor slab. ANO engineering also conservatively redefined the total deadweight of all the racks, and included 5000 lb contingency loads between each rack and the pool walls around the periphery of the pool, (60,000 lb total), to account for miscellaneous items stored in this area of the pool. Additionally, a conservative hydrodynamic pressure resulting from the seismic displacement of the racks was specified, which loads the pool walls for the height of the racks.